NUMERICAL STUDY ON SEISMIC RESPONSE OF ROOF-TOP MOUNTED COOLING TOWER

S. Saranya[1] & P. Sunitha[2]

[1] Doctoral Research Student, EERC, IIIT Hyderabad, India, saranya.s@research.iiit.ac.in

[2] Assistant Professor, EERC, IIIT Hyderabad, India

Abstract: *Cooling towers are commonly used in commercial, industrial, and hospital buildings for Heating, Ventilating, and Air Conditioning requirements. In general, they are mounted on roof of buildings and designed as Non-Structural Elements (NSE). Further, for minimum transfer of vibrations during strong earthquake shaking to the supporting buildings, vibration isolators are used. While experimental test results provide realistic seismic demand estimates, numerical analysis help predict demands reasonably well if numerical modelling and nonlinear analysis are carried out using realistic assumptions of structure and its behaviour. This study is an attempt in this direction, considers a cooling tower from past shake table test, and presents numerical modelling and pertaining seismic response investigations. For the numerical study, complete coupled modelling (cooling tower and the building modelled together) is carried out in commercial software SAP2000, and decoupled modelling (cooling tower only) in ABAQUS. And, nonlinear time history analysis is performed to estimate component amplification factor, peak shear force, peak axial force, maximum relative displacements, and roof acceleration response history. Several outcomes were closely matched with the experimental results. However, significant variation is observed in some of the seismic demands, which can be attributed to assumptions made in numerical modelling.*

Keywords: Cooling tower, NSE, fundamental period, Component Amplification Factor, anchor bolts.

1. Introduction

Non-structural elements (NSEs) of a building include all building contents except those regarded as part of the lateral-load resisting systems, namely beams, columns, slabs, braces, and structural walls. NSEs account for approximately 82%, 87%, and 92% of the total construction cost in office, hotel, and hospital buildings, respectively (Whittaker and Soong, 2003). In general, NSEs can be broadly classified into three categories, namely:(i) architectural components, (ii) mechanical, electrical, and plumbing components, and (iii) furniture, fixtures, and equipments (FEMA E-74, 2012). Of these, mechanical components such as cooling towers and centrifugal chillers are essential for maintaining the continuity of building services post-earthquake, in critical buildings. These NSEs are commonly mounted on the roof and supported on vibration isolators to minimize the vibration transferred to the primary structure. Failure of these NSEs can cause significant downtime, financial loss, and even fatalities. For example, inadequately anchored roof-mounted NSEs sustained severe damages in the 2001 Kutch, 2010 Chile and 2014 South Napa earthquakes compared to NSEs elsewhere in the buildings (Bose *et al*., 2004; FEMA E-74, 2012; NIST GCR 17-917-44, 2017). This confirms the need to adequately design anchorages of NSEs also. These failures primarily result from the dynamic interaction between Structural Elements (SE) and Non-Structural Elements, which are usually not considered during numerical modelling and design. Also, at the same fundamental frequency of NSE and building, maximum response is observed when the NSE is mounted on roof (Hadjian, 1977). The dynamic interaction is difficult to determine without experimental investigations, and the presence of a wide variety of NSEs further adds complexity. Performance of mechanical components, such as centrifugal chillers and diesel generator mounted on vibration isolators was experimentally tested on shake table (Figure 1; Fathali *et al*., 2008; Lin *et al*., 2011). Experimental results indicated that in most cases, the component amplification factor (ratio of peak component acceleration demand to peak floor acceleration demand) exceeded the code recommended value of 2.5 for the equipment mounted on vibration isolators (ASCE 07, 2016).

(a)

(b)

*Figure 1: (a) Chiller, and (b) diesel generator, mounted on vibration isolators (*Fathali *et al*., 2008; Lin *et al*., 2011)

However, the dynamic interaction and equipment connections with supporting structure were not simulated in these tests. Later, full-scale building experiments with limited NSEs was conducted to study the dynamic interaction of NSEs with supporting structure (Furukawa *et al*., 2013; Duozhi *et al*., 2016; Bianchi *et al*., 2020; Dhakal *et al*., 2020). Further, it was observed that the use of Viscous Wall Dampers in a 15-storey hospital building resulted in: (a) reduction of force demand on acceleration-sensitive NSEs, (b) improvement in performance of NSEs by limiting damage, and (c) minimisation of NSEs bracing costs (Newell *et al*., 2011). Also, a base-isolated five-storey steel frame demonstrated damages to integrated suspended ceiling partitions and wall-sprinkler piping systems (Ryan *et al*., 2015). In addition, results from nonlinear finite element modelling and response simulation of a five-storey reinforced concrete (RC) building along with a broad range of idealised NSEs, namely (a) passenger elevator, (b) prefabricated metal stairs, (c) façade, (d) interior furnishings, (e) mechanical and electrical subsystems, (f) medical equipments, and (g) roof-mounted air handling units, penthouse, and cooling tower, were used as pretest response to conduct shake table tests of full scale model (Ebrahimian *et al*., 2018). From the above, seismic response of the cooling tower mounted on the base-isolated (BI) and fixed-base (FB) conditions of building was investigated (Astroza *et al*., 2015); this study with FB building is numerically investigated in detail in this paper.

2. Numerical Study

The following numerical models are developed in this study. Firstly, in commercial software SAP2000, (a) Complete coupled modelling (cooling tower and the building modelled together) for preliminary linear and nonlinear analysis, (b) decoupled modelling (cooling tower only) for matching the fundamental period of NSE in numerical model and experiment. Secondly, in finite element software ABAQUS, cooling tower and connections subjected to roof acceleration response history from SAP2000, are modelled.

2.1. Details of the RC building

Five storey RC study building was located in Southern California and founded on stiff soil. The estimated total weight of the bare structure was 3010 kN, and 4420 kN with NSE. For columns and elevator shear walls 40 MPa concrete (cylinder strength) and 35 MPa concrete for beams and slabs were used. Each floor was composed of typical NSEs to simulate various occupancies. Typical storey height was 4.27m. Two openings accommodated full-height elevator and stair shafts (Figure 2). Structural walls enclosing elevators in N-S direction and cross bracings on opposite peripheral bays were also provided at all storeys (Figure 5(b)). The building was designed to withstand 2.5% maximum lateral interstorey drift, 3.5% ultimate interstorey drift, and 0.7g-0.8g maximum peak floor acceleration (Ebrahimian *et al*., 2018; Chen *et al*., 2016).

2.2. Details of the Cooling Tower

Cooling tower mounted on a W8x18 steel base frame supported by four isolation/restraint (I/R) in the N-E corner building roof measured 2.73 m × 2.14 m in plan and 3.25 m tall. (Figure 3, 4(a) & (b)). Axial stiffness, and horizontal stiffness of springs of I/R assembly are also accounted for. The I/R devices consists of two components namely, (a) isolation component and, (b) restraint component (Figure 4(c)). The total weight of cooling tower is 15.6 kN and 27.9 kN, in empty and operational conditions, respectively. Design component amplification factor and response reduction factor were 2.5 and 2.0, respectively (Astroza *et al*., 2015; Chen *et al*., 2016).

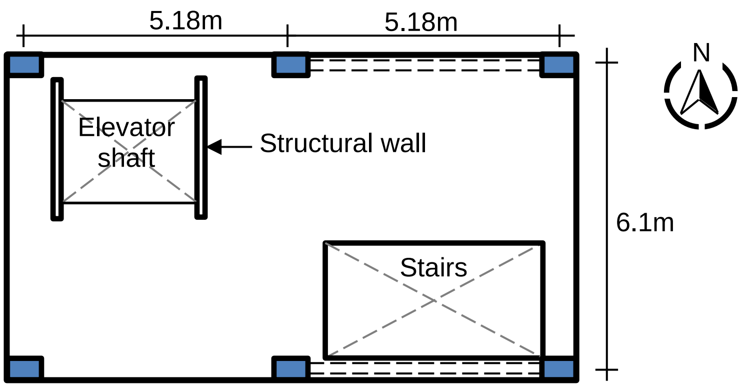

Figure 2: Schematic plan view – Typical floor (Adapted from Astroza *et al*., 2015)

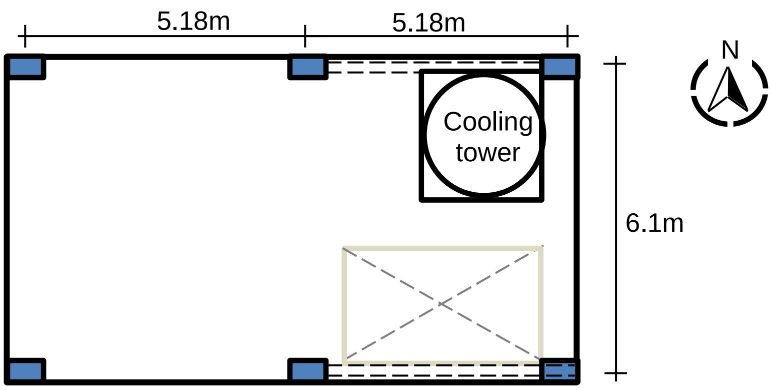

Figure 3: Schematic plan view – Roof (Adapted from Astroza *et al*., 2015)

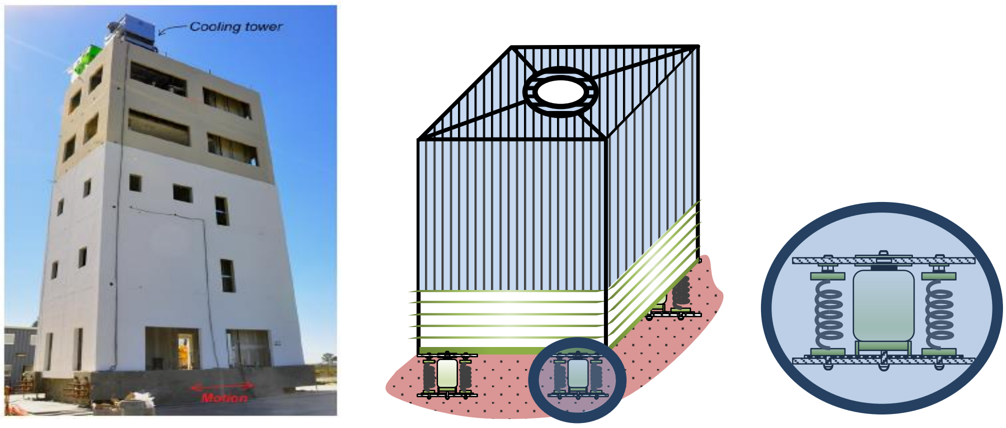

(a) (b) (c)

*Figure 4: (a) Complete building with cooling tower at roof (*Astroza *et al*., 2015)*, (b) Schematic cooling tower, and (c) Vibration isolator*

2.3. Details of Numerical Modelling

In SAP 2000, the masses of the exterior facade and precast concrete cladding panels were distributed to the perimeter nodes based on tributary lengths in the building (Wang *et al*., 2013), while the masses of the remaining NSEs were distributed uniformly to the tributary nodes at each floor. Mander's confinement model is used for concrete modelling, and shell elements for structural walls, slabs, and cooling tower (Figure 5(a) & 5(b)). Plastic hinges are defined in select members of the building to model nonlinearity. Three dimensional base plates are modelled using solid finite elements. Solid elements are commonly used to model 3D structures, and it activates the three translational degrees of freedom at each of its connected joints (CSI, 2016). Isolators are modelled using spring elements, and cooling tower attached to roof slab by equal displacement constraint in SAP2000.

In ABAQUS sub-assemblage model, (Figure 5(c)), concrete damage plasticity model for concrete and elasto-plastic model for steel is used. 8-node hexahedral element with reduced integration and hourglass control (C3D8R) is used for meshing for all parts, and tie constraint for baseplate-steel frame & steel frame-cooling tower contact interfaces. Surface-to-surface contact interaction is applied to base plate-bolt, base plate-concrete, and concrete-bolt contact interfaces (cohesive interaction). HARD contact was used for normal behaviour towards the interface plane, and PENALTY option was adopted for the tangential behaviour. Friction coefficients between concrete and steel was taken to be 0.4 and 0.3 for all other interactions (Guo *et al*., 2020; Chen *et al*., 2019). Spring elements are used to model the isolators. Modelling of I/R assembly and anchor bolts (HSL-3-G) is carried out as per the specifications given in the reference (Astroza *et al*., 2013). Effects of openings, snubbers of I/R assembly, load cells, and water sloshing effects are neglected in the numerical modelling; only the opening on top part of cooling tower is considered, which affects dynamic characteristics insignificantly. Thus, in SAP2000 model above, this opening is not simulated.

3. Ground Motion Characteristics used for Nonlinear Time History Analysis

The 2007 Pisco earthquake ground motion (Ebrahimian *et al*., 2018; ACELDAT-PERÚ; Alarcón, 2008) used in experiment (FB4-ICA100) is considered for numerical analysis (Figure 6). Total duration and peak ground acceleration of the ground motion are 160s and 0.26g, respectively. And, to reduce the computational time in ABAQUS, the study considered the strong motion duration defined as the time interval between 5%-95% of the Arias intensity (Arias, 1970); the integral of ground acceleration is given as:

$$I_A = \frac{\pi}{2g}\int_0^{T_D} [\ddot{x}(t)]^2 \, dt \quad (1)$$

where $\ddot{x}(t)$ is ground acceleration, *g* acceleration due to gravity, and T_D total duration of earthquake. Rayleigh damping is used to simulate the damping characteristics. For the nonlinear time history analysis unscaled ground motion is used as in the shake table test.

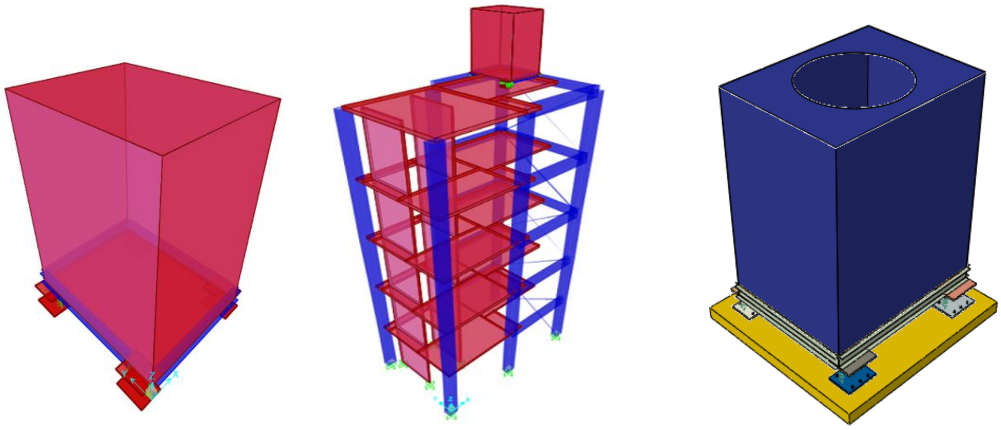

(a) (b) (c)

Figure 5: (a) Cooling tower model in SAP 2000, (b) Complete model in SAP 2000, (c) Cooling tower model in ABAQUS

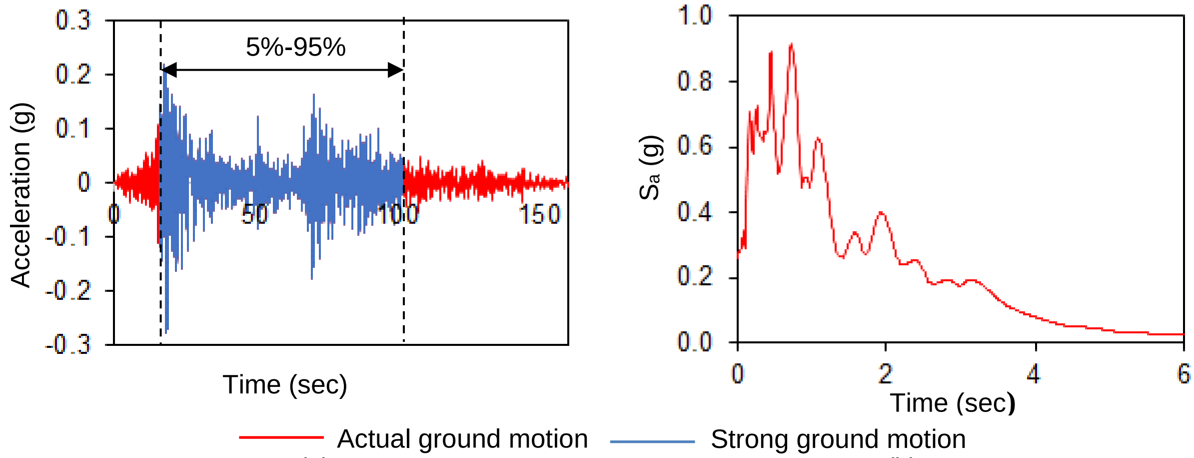

(a) (b)

Figure 6: (a) Acceleration time history of the ground motion, (b) Elastic acceleration response spectrum of the ground motion

4. Discussion of results

4.1. Modal properties

Firstly, the E-W modal property of the building from SAP2000 are confirmed to match with reference values from Opensees and Diana softwares and measured from white noise test of experimental model (Table 1) (Wang *et al*., 2013). Only E-W direction is considered in the current study because ground motion is applied along this direction in shake table test. (Figure 7).

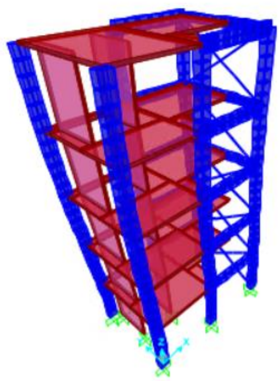

Figure 7: Fundamental mode of building

Table 1: Modal properties of building

Mode	Direction	Fundamental period (sec)			
		Opensees (Reference)	Diana (Reference)	Shake Table (Experimental Study)	SAP 2000 (Current Study)
1	E-W	0.71	0.71	0.74	0.71

Likewise, the modal properties of the cooling tower from SAP2000 and ABAQUS are confirmed to match from white noise test results (Table 2 & Figures 8 and 9) (Astroza *et al*., 2015). Minor variation can be attributed to assumptions made in numerical modelling. First mode is in the vertical direction due to the least stiffness, when compared to the horizontal directions.

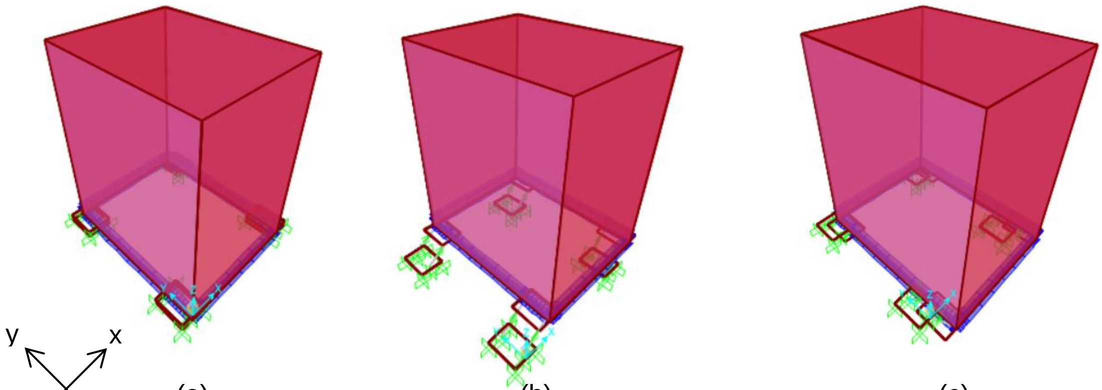

(a) (b) (c)

Figure 8: SAP 2000 :(a) Mode 1, (b) Mode 2, and (c) Mode 3

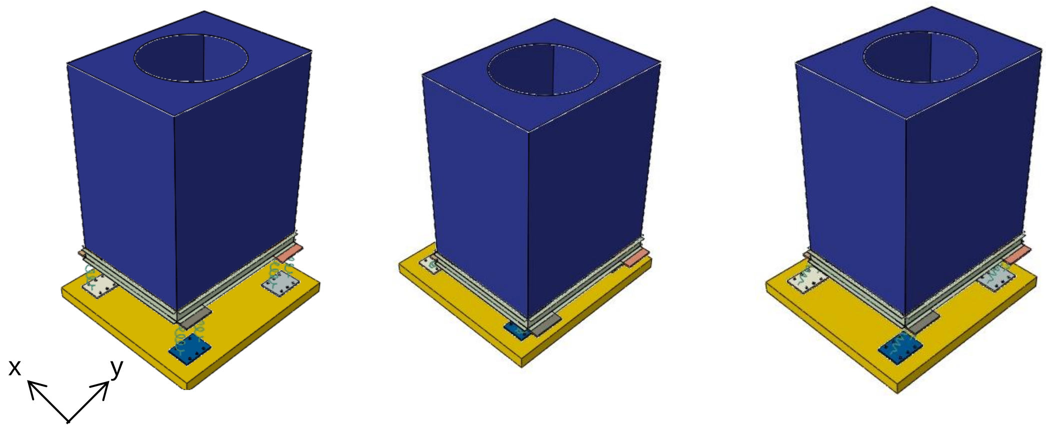

(a) (b) (c)

Figure 9: ABAQUS :(a) Mode 1, (b) Mode 2, and (c) Mode 3

Table 2: Modal properties of cooling tower

Mode	Direction	Fundamental period (sec)		
		White Noise Test (Experimental Study)	SAP 2000 (Decoupled model)	ABAQUS (Sub-assemblage model)
1	UD	0.21	0.31	0.33
2	E-W	0.18	0.29	0.32
3	N-S	0.15	0.29	0.32

4.2. Structural Response

Peak Floor Acceleration (PFA) obtained from the numerical investigations is compared with the experimental results (Ebrahimian *et al*., 2018). PFA agrees closely with the measured values at all floors, except floor 2 (Figure 10 (a)). At floor 1, the PFA is 0.30g and -0.29g, 0.45g and -0.41g at floor 2, 0.52g and -0.55g at floor 4, and 0.64g and -0.58g at floor 5. As expected, and demonstrated in experiment, PFA is maximum towards upper floors.

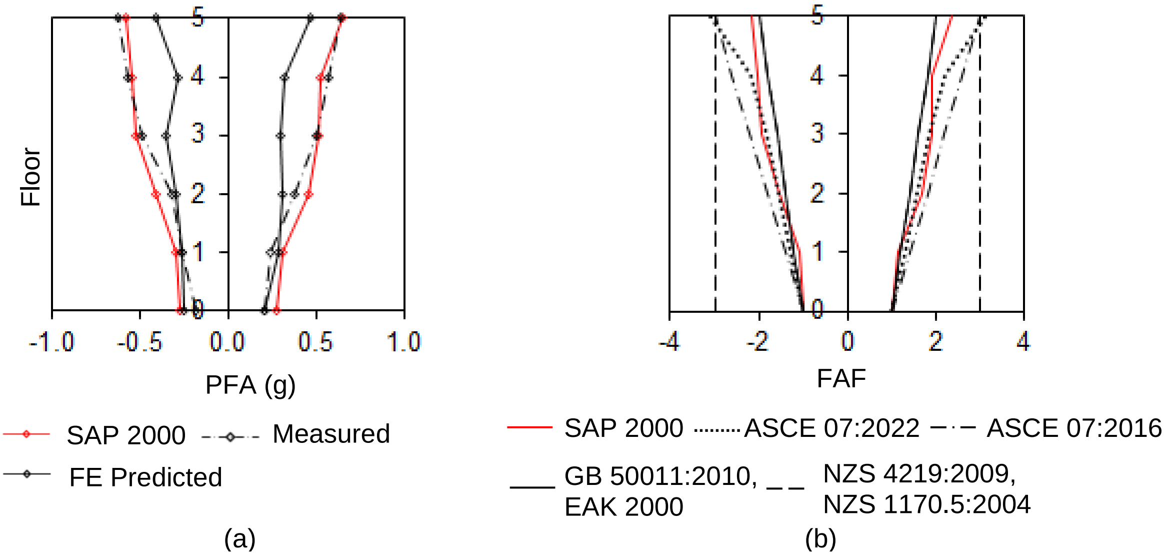

Figure 10: (a) Variation of Peak Floor Acceleration, and (b) Variation of Floor Amplification Factor

Further, Floor Amplification Factor is determined, which is the ratio of Peak Floor Acceleration (PFA) to Peak Ground Acceleration (PGA) representing dynamic amplification of acceleration from the ground to the floor where NSE is mounted (Figure 10(b)). It is observed that the variation of FAF is not having a constant slope as stipulated by the international codes (EAK 2000; GB50011-2010; ASCE 07-2016; NZS 1170.5-2004; NZS 4219-2009). FAF estimated using EAK 2000 and GB 50011:2010 predicted lesser FAF, nearly identical FAF at lower and intermediate floors using ASCE 07:2022, and higher FAF using ASCE 07:2016, NZS 4219:2009, and NZS 1170.5:2004, compared to numerical results. Similarly, Peak Interstorey Drift Ratio (PIDR) values from pre-test nonlinear finite element modelling and numerical results are closer (Figure 11) (Ebrahimian *et al*., 2018); PIDR is maximum in the intermediate floor and minimum at the top floors, usually expected in regular low-rise buildings. They are, 0.23% and -0.23% between floor 4 and 5, and 0.75% and -0.85% between floor 2 and 3. Nevertheless, the experimental PIDR results are far off from the FE and SAP 2000 predicted values. This can be attributed to not accounting for stiffness contribution of NSEs during design of the structure, used in FE and SAP2000 numerical investigations. This observation further reinforces the importance of adopting *complete modelling* method of SE-NSE in buildings.

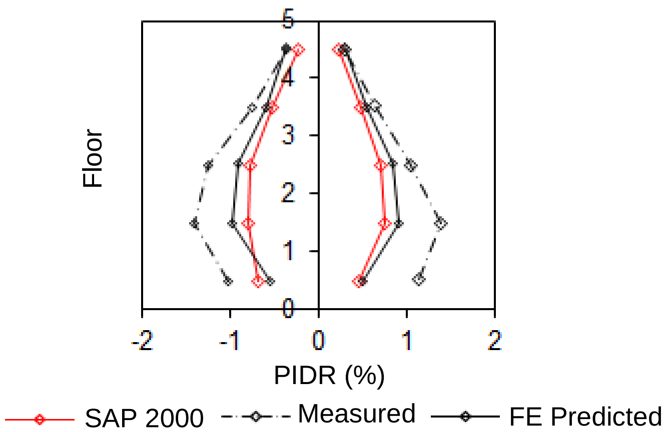

Figure 11: Variation of PIDR

4.3. Component Amplification Factor

Component Amplification Factor (CAF) represents the dynamic amplification of acceleration from the floor where NSE is mounted to the top of the NSE, here at the top of the cooling tower. Mathematically, it is the ratio of Peak Component Acceleration (PCA) to Peak Floor Acceleration (PFA). While CAF is evaluated from SAP 2000 from the complete model, in ABAQUS, Acceleration Floor Response Spectrum (AFRS) approach is adopted (Oropeza *et al*., 2010). In this approach, the extracted roof acceleration response history from SAP 2000, curtailed for significant duration is given as input to cooling tower model in ABAQUS, and the acceleration response history at the top the cooling tower obtained. The CAF estimated from SAP2000 complete model, ABAQUS cooling tower (alone) model and measured from shake table test are presented in Table 3. Only values in E-W direction are listed, as the ground motion is applied in this direction in complete model and shake table, and subsequently the input acceleration response history (for significant duration) in ABAQUS also in E-W direction of cooling tower.

Further, 5% damped acceleration *response spectrum* for the 2 acceleration response histories from SAP 2000 -obtained at roof and top of the cooling tower, is presented (Figure 12), to understand any possible amplification close to fundamental period of cooling tower. As expected, response amplification is observed close to 0.8s, and hence near maximum of 5.4g at top of cooling tower is observed close to 0.71s, the fundamental period of the building. Similarly, response amplification at roof is observed between 0.55-0.75s, and hence a near maximum value of 4g close to 0.71s. In addition, CAF suggested by ASCE 07:2016 and ASCE 07:2022 considers the *mounting assembly types* also. For *eg*., for the equipment mounted on vibration isolator (similar to that used in shake table test considered in this paper), CAF recommended by the above 2 codes are 2.5 and 2.2, respectively. But, NZS 1170.5 :2004 suggests a value based on *fundamental period of NSE* to be 2 for the fundamental period of the NSE less than 0.75s, and EAK 2000 suggests CAF of 1.34 and considers *fundamental period of both NSE and SE*. Thus, design documents consider different characteristics of NSE and SE, while stipulating the CAF values (Table 4). The obtained CAF demands from present numerical investigations (in this paper) and measured values from shake table test are well below the ASCE and NZS code values mentioned above, but exceeds the value recommended by EAK 2000.

Table 3: Component Amplification Factor

Direction	**Shake Table (Experimental Study)**	**SAP 2000 (Complete model)**	**ABAQUS (Sub-assemblage model)**
E-W	≈1.7	1.4	1.7

Table 4: Characteristics of SE and NSE recommended by codes for estimating CAF

Codes	**Support conditions**	**Fundamental period of NSE**	**Fundamental period of building**	**Building typology**
ASCE 07:2016	✓	✓	✓	…
ASCE 07:2022	✓	✓	✓	…
EAK 2000	…	✓	✓	…
NZS 1170.5:2004	…	✓	…	…
NZS 4219:2009	…	…	…	…
EN 1998.1:2004	…	✓	✓	…
GB 50011:2010	✓	…	…	✓

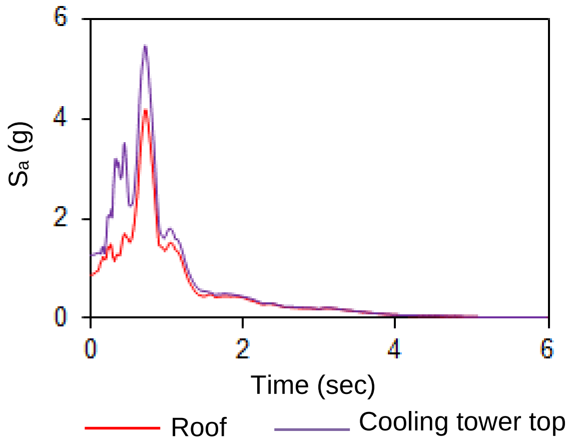

Figure 12: Roof and Component Acceleration response spectrum from floor acceleration time history

4.4. Force and Displacement Demands

Table 5 compares numerical values of peak shear force and peak axial force demands obtained from experiment with values obtained from SAP2000 and ABAQUS, and Figure 13 shows the corresponding response history records during strong motion duration. It is observed that peak shear force demand from SAP 2000 matches the experimental demand. The higher peak shear force demand from ABAQUS could be attributed to decoupled modelling used. Significant variation is observed in the peak axial force, which can be attributed to simplifying assumptions made in numerical modelling, especially shortcomings in connection simulations. Thus, it is recommended that SE-NSE be modelled together (complete modelling) to closely simulate the actual behaviour of both and later use the floor response as demands to a detailed NSE sub-assemblage model. Complete modelling will be more critical for the above analysis if the weight of NSE is significantly comparable to the weight of SE; for eg., ASCE 07 (2022) recommends considering the component as NSE if the weight is less than 20% of seismic weight of SE. If NSE weight is more than 20% of the structure, the component must not be considered as NSE, but as non-building component.

Table 5: Force Demands

Peak Shear Force, kN			**Peak Axial Force, kN**		
Shake Table (Experimental Study)	**SAP 2000 (Complete model)**	**ABAQUS (Sub-assemblage model)**	**Shake Table (Experimental Study)**	**SAP 2000 (Complete model)**	**ABAQUS (Sub-assemblage model)**
≈ 7.0	7.1	9.3	≈ 14.0	5.8	12.4

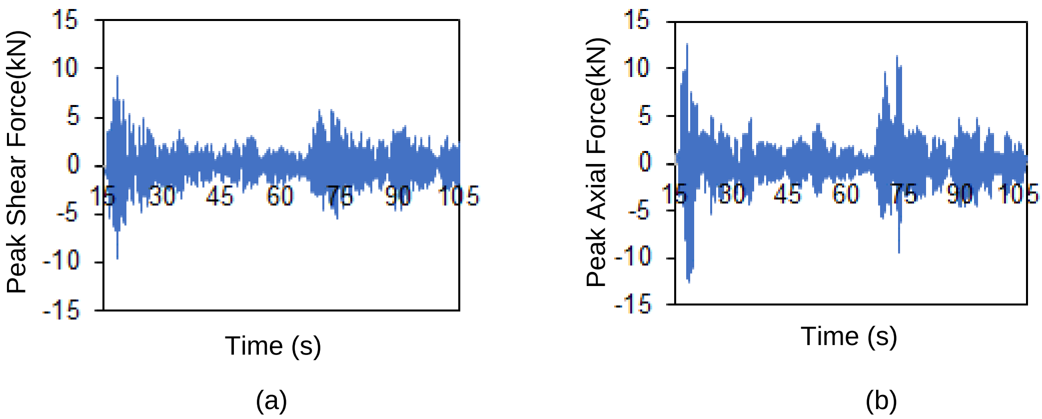

Figure 13: (a) Variation of Peak Shear force, and (b) Variation of Peak Axial Force

Finally, the maximum displacement in the direction of shaking between the roof slab where cooling tower is mounted and the tower base formed on top of the W8x18 frame was compared to the experimental results (Astroza *et al*.,2015); the displacements are 7.5mm, 8mm, and 6mm, from experiment, SAP2000, and ABAQUS, respectively. This close agreement provides confidence in the numerical modelling adopted in this study.

4.5. Connections

HILTI HSL -3G M16 Anchor bolts are used as per the specifications (HILTI, 2018) to connect base plate of the cooling tower with roof. It was observed that only 0.2% of finite elements defining the bolt have plastified in the inner bolt core. Remaining bolts remained elastic state. Stress concentrations near the bottom of the bolt and in the washer-bolt interface are visible from the Von Mises stress distribution (Figure 14(a)). Likewise, base plates also remained elastic, with higher stress concentration near the bolt holes (Figure 14 (b)). No failures in the bolt and base plate are observed under shear and tensile forces. This finding aligns with the experimental observations (Astroza *et al*., 2015).

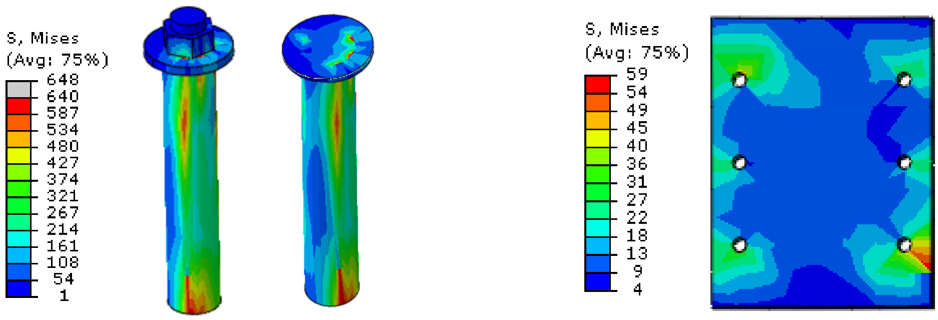

(a) (b)

Figure 14: Von Mises stress distribution: (a) bolt, and (b) base plate

5. Conclusions

This study attempted to numerically simulate the cooling tower response of a past shake table test set up, by adopting a complete coupled modelling of building and cooling tower together and decoupled modelling of cooling tower with connections. From the numerical investigations the following salient dynamic characteristics, component characteristics and force demands, and connections of SE-NSE, closely matches with white noise test results and experimental values. They are: (i) the fundamental period of the cooling tower (~0.11s) alongside oscillation directions and fundamental period of building, (ii) PFA across height of buildings (~0.05g at roof) and CAF of cooling tower (~0.15), (iii) maximum relative displacement between the roof and at the bottom of the cooling tower in E-W direction (~0.50mm), (iv) peak shear force (~1.20kN), and (v) connections of cooling tower. In the above, average values are listed. The above observations help draw the following conclusions:

1. coupled modelling and decoupled modelling approaches used in the study for numerical investigations can be used to help predict the seismic demands and seismic behaviour of similar SE-NSE, subjected to strong earthquake shaking reasonably well;
2. finite element modelling of cooling tower and its connections performed in this study can be used to examine the failure modes of connections in detail, especially for ductile and brittle modes of failures; and
3. numerical simulations employing appropriate modelling of SE-NSE similar to that carried out in this work help adopt suitable design precautions to ensure seismic safety of NSEs, which is more critical in important buildings like hospitals.

6. References

ACELDAT-PERÚ, Geophysical institute of Peru https://www.igp.gob.pe/servicios/aceldat-peru

Alarcón J.E., Taucer F., So E. (2008). The 15 August 2007 Pisco, Peru, earthquake-post-earthquake field survey, *Proceedings of the 14th World Conference on Earthquake Engineering,* Beijing, China.

Arias A. (1970). A measure of earthquake intensity. Seismic Design for Nuclear Power Plants, Hansen RJ, (editor), Cambridge, Massachusetts: MIT Press, 23, 438-483.

ASCE/SEI 07 (2016). *Minimum design loads and associated criteria for buildings and other structures*, American Society of Civil Engineers/Structural Engineering Institute, Reston.

ASCE/SEI 07 (2022). *Minimum design loads and associated criteria for buildings and other structures*, American Society of Civil Engineers/Structural Engineering Institute, Reston.

Astroza R., Pantoli E., Selva F., Restrepo J. I., Hutchinson T. C., Conte J. P. (2013). Experimental evaluation of the seismic response of a rooftop-mounted cooling tower, Structural Systems Research project, Report No. SSRP-13/14, University of California, San Diego.

Astroza R., Pantoli E., Selva F., Restrepo J. I., Hutchinson T. C., Conte J. P. (2015). Experimental evaluation of the seismic response of a rooftop-mounted cooling tower, *Earthquake Spectra*, 31(3): 1567-1589.

Bianchi S., Ciurlanti J., Perrone D., Pampanin S., Filiatrault A. (2020). Seismic demand and performance evaluation of non-structural elements in a low-damage building system, *Proceedings of the 17th World Conference on Earthquake Engineering*, Sendai, Japan.

Bose A., Bose P. R., Sinvhal A., Verma A., Khan A. A. (2004). Impact of Kutch earthquake on non-structural elements and appendages of buildings, *Proceedings of the 13th World Conference on Earthquake Engineering*, Vancouver, Canada.

CEN (2004). EN 1998-1:2004. Eurocode 8*: Design of structures for earthquake resistance - Part 1: General rules, seismic actions and rules for buildings*, Comité Européen de Normalisation, Brussels.

Chen J., Wang W., Ding F. X., Xiang P., Yu Y. J., Liu X. M., *et al*. (2019). Behavior of an advanced bolted shear connector in prefabricated steel-concrete composite beams, *Materials*, 12(18): 2958.

Chen M. C., Pantoli E., Wang X., Astroza R., Ebrahimian H., Hutchinson T. C., *et al*. (2016). Full-scale structural and nonstructural building system performance during earthquakes: Part I–specimen description, test protocol, and structural response, *Earthquake Spectra*, 32(2): 737-770.

Chen M., Pantoli E., Wang X., Espino E., Mintz S., Conte J., Hutchinson T., Marin C., Meacham B., Restrepo J., Walsh K. (2012). Design and construction of a full-scale 5-story base isolated building outfitted with nonstructural components for earthquake testing at the UCSD-NEES facility, *Structures Congress*, 1349-1360.

CSI (2016). Analysis Reference Manual for SAP 2000, ETABS, SAFE and CSiBridge, California, USA.

Dhakal R., Rashid M., Bhatta J., Chen C., Song G., Sullivan, T., *et al*. (2020). Shake table testing plan for multiple non-structural elements & contents in a low–damage structural steel building, *Proceedings of the 17th World Conference on Earthquake Engineering*, Sendai, Japan.

Duozhi W., Junwu D., Xiaoqing N. (2016). Shaking table tests of typical b-ultrasound model hospital room in a simulation of the Lushan earthquake. *Bulletin of the New Zealand Society for Earthquake Engineering,* 49(1): 116-124.

EAK (2000). *Code for Seismic Resistant Structures*, Earthquake Planning and Protection Organization, Athens, Greece.

Ebrahimian H., Astroza R., Conte J. P., Hutchinson T.C. (2018). Pretest nonlinear finite-element modelling and response simulation of a full-scale 5-story reinforced concrete building tested on the NEES-UCSD shake table, *Journal of Structural Engineering*, 144(3): 04018009.

Fathali S., Filiatrault A. (2008). Effect of elastomeric snubber properties on seismic response of vibration-isolated mechanical equipment: An experimental study, *Earthquake Spectra*, 24(2): 387-403.

FEMA E-74 (2012). Reducing the risks of nonstructural earthquake damage—a practical guide. Federal Emergency Management Agency, Washington DC.

Furukawa S., Sato E., Shi Y., Becker T., Nakashima M. (2013). Full-scale shaking table test of a base-isolated medical facility subjected to vertical motions, *Earthquake Engineering & Structural Dynamics,* 42(13): 1931–1949.

GB50011 (2010). *Code for Seismic Design of Buildings*, National Standard of the People's Republic of China, Beijing, China.

Guo Q., Chen Q. W., Xing Y., Xu Y. N., Zhu Y. (2020). Experimental study of friction resistance between steel and concrete in prefabricated composite beam with high-strength frictional bolt, *Advances in Materials science and Engineering*, 1-13.

Hadjian AH. (1977). On the Decoupling of Secondary Systems for Seismic Analysis, *Proceedings of the 6th World Conference on Earthquake Engineering,* New Delhi, India.

HILTI. (2018). HSL-3/HSL-3-R EXPANSION ANCHOR, Technical datasheet.

Lin F.R., Cheng C.W., Chen M.F., Wang S.J., Hwang J.S., Chang K.C. (2011). Full-scale experimental study on seismic behavior of vibration isolated mechanical/electrical equipment, *Proceedings of the 9th Pacific Conference on Earthquake Engineering*, Auckland, New Zealand.

Newell J., Love J., Sinclair M., Chen Y.N., Kasalanati A. (2011). Seismic design of a 15-story hospital using viscous wall dampers, *Proceedings of Structures Congress*, Las Vegas, NV, USA.

NIST GCR 17-917-44 (2017). Seismic analysis, design, and installation of nonstructural components and systems—background and recommendations for future work. National Institute of Standards and Technology, Gaithersburg.

NZS 1170.5 (2004). *Structural design actions Part 5: Earthquake actions, Standards New Zealand*, Wellington, New Zealand.

NZS 4219 (2009). *Seismic performance of engineering systems in buildings*, Standards New Zealand, Wellington, New Zealand.

Oropeza M., Favez P., Lestuzzi P. (2010). Seismic response of nonstructural components in case of nonlinear structures based on floor response spectra method, *Bulletin of earthquake engineering*, 8(2): 387-400.

Ryan K.L., Soroushian S., Maragakis E.M., Sato E., Sasaki T., Okazaki T. (2015). Seismic simulation of an integrated ceiling-partition wall-piping system at E-Defense. I: Three-dimensional structural response and base isolation, *Journal of Structural Engineering*, 142(2): 04015130.

Wang X., Ebrahimian H., Astroza R., Conte J.P., Restrepo J.I., Hutchinson T.C. (2013). Shake table testing of a full-scale five-story building: pre-test simulation of the test building and development of an NCS design criteria, ASCE, *Structures Congress*,1460-1471.

Whittaker A.S., Soong T.T. (2003). An overview of nonstructural component research at three U.S. earthquake engineering research centers, *Proceedings of Seminar on Seismic Design, Performance, and Retrofit of Nonstructural Components in Critical Facilities*, Applied Technology Council, ATC-29-2, Redwood City, California.